# A MICROSTRUCTURE DESCRIPTION OF THE RELATIONSHIP BETWEEN FORMATION RESISTIVITY FACTOR AND POROSITY

Carl Fredrik Berg
Statoil ASA

*This paper was prepared for presentation at the International Symposium of the Society of Core Analysts held in Napa Valley, California, USA, 16-19 September, 2013*

## ABSTRACT

The formation resistivity factor evaluation of brine-filled reservoir rock is an essential part of electrical resistivity log interpretation in petroleum exploration. Empirical relations such as Archie's law are widely employed to model the relationship between the formation resistivity factor and porosity. Historically, the Archie cementation exponent has been obtained from experimental laboratory measurements. Nowadays, it is possible to approach the formation resistivity factor via numerical calculation on digital images of the microstructure of the reservoir rock.

In this paper, we give a direct microstructure description of the relationship between the formation resistivity factor and the porosity, instead of the Archie cementation exponent typically derived from core plug measurements. The pore microstructure effect is defined by a tortuosity and a constriction factor. The combined effect of the calculated tortuosity and constriction, in addition to the porosity, yields the effective formation resistivity factor.

To demonstrate the theory we calculate the tortuosity and constriction factor for digital rock images and models of Fontainebleau sandstone, and thereby obtain a microstructure-related correlation between porosity and the formation resistivity factor in agreement with published experimental data. Such tortuosity and constriction factors provide useful fundamental microstructure parameters allowing evaluation of the pore structure representation in digital rock modeling.

## INTRODUCTION

In this paper, we will investigate the electrical conductivity of a clay-free sedimentary rock filled with brine, where the rock matrix is assumed insulating and the electrical conductivity of the brine is assumed constant. The electrical conductance of the rock is dependent on the porosity and pore microstructure relative to the applied potential.

The formation resistivity factor *FRF* is defined to be the ratio of the electrical resistivity of the rock saturated with brine $R_o$ to the resistivity of the brine $R_w$:

$$FRF = \frac{R_o}{R_w}. \quad (1)$$

In his seminal paper [1], Archie formulated an empirical relationship between the formation resistivity factor *FRF* and the porosity $\varphi$ of sandstones, given by the equation

$$FRF = \varphi^{-m}, \tag{2}$$

where *m* is called cementation exponent. In [2], the formation factor is re-formulated as

$$FRF = \frac{C_c}{\varphi_c \tau_c^2}. \tag{3}$$

Here, $\tau_c$ is a tortuosity, $C_c$ is a constriction factor, and $\varphi_c$ is the part of the pore space conducting electricity. Thus, the formation resistivity factor *FRF* is decomposed into descriptors of the pore structure.

In this paper, we will calculate the tortuosity $\tau_c$, constriction factor $C_c$ and porosity $\varphi_c$ from microtomography (micro-CT) images and models of Fontainebleau sandstones. The parameters will be determined both directly on the voxel based images and on pore network representations.

## BACKGROUND

Consider a brine filled, clay-free sandstone with an applied electrical potential $\Delta U$ over two opposite end-planes of the sample. Then the local electrostatic potential *U* satisfies Laplace's equation

$$\nabla^2 U = 0, \tag{4}$$

with the boundary condition $\nabla U \cdot \vec{n} = 0$ for the unit normal $\vec{n}$ on the grain surface. The rate of energy applied to the system is $I_t \Delta U$, were $I_t$ is the total electrical current through the sample. The applied energy is used to conduct current from inlet to outlet. For a given porosity, the optimal pore geometry for conducting electricity is a set of tubes from inlet to outlet of constant cross sectional area and length equal the length of the sample. For such an optimal geometry, the electrostatic field $E = -\nabla U$ is the constant $-\Delta U/S$, where $S$ is the length of the sample.

Other geometries of the pore space will result in increased resistance: Longer electric field lines ("streamlines" of the current) result in less conductance given the same applied electrical potential, reflected in a smaller electrostatic field value $E = -\nabla U$. This increased resistance is measured as a tortuosity. Also energy is expended on variation in the magnitude of the electrostatic field, which is measured as a constriction factor.

The tortuosity of a path is the ratio between the distance *l* between the end points of the path and the path length *s*: $\tau = l/s$ [3]. For a porous medium, several definitions exist for the tortuosity. Following [2], we define tortuosity as

$$\tau_c^2 = \frac{1}{\Omega_c} \int_P \tau(\Gamma)^2 d\Gamma. \tag{5}$$

Here $P$ is the set of electric field lines in the porous medium, $\Omega_c$ is the subset of the pore space spanned by the electric field lines in $P$, and $\tau(\Gamma) = S/l_\Gamma$ is the tortuosity of the

electric field line Γ of length $l_\Gamma$. The tortuosity has a maximal value of 1, which is reached when all electric field lines have a length equal the length $S$ of our porous medium. Longer electric field lines give a smaller tortuosity and thereby a larger formation factor in Equation (3). Hence, longer electric field lines reduce the efficiency of the porous medium to conduct electricity.

Note that neither the value for the conductivity $\sigma$ of the brine, nor the applied voltage drop $\Delta U$ affects the tortuosity $\tau_c$ , thus the tortuosity is only dependent on the pore structure and the direction of the voltage drop.

The drift velocity $v=\mu E$ of the current is proportional to the electrostatic field $E$. When the electric current passes through a constriction, the drift velocity is increased. Variation in pore size thus translates into a variation in drift velocity. For varying drift velocity, energy is expended, and the effectiveness of the pore space to conduct flow is reduced. Following [2], we define the constriction factor $C(\Gamma)$ for an electric field line Γ as

$$C(\Gamma) = \frac{1}{l_\Gamma^2}\int_\Gamma |E(s)|ds \int_\Gamma \frac{1}{|E(s)|}ds = \frac{1}{l_\Gamma^2}\Delta U \int_\Gamma \frac{1}{|E(s)|}ds. \qquad (6)$$

The constriction factor $C_c$ for the porous medium is then the current weighted average of the constriction factors for the electric field lines:

$$C_c = \frac{1}{I_t}\int_P C(\Gamma)dI_\Gamma. \qquad (7)$$

The constriction factor has a minimal value of 1, reached when the electrostatic field, equivalently the drift velocity, is constant along each field line. Larger variation in the electrostatic field increases the constriction factor and thereby the formation factor in Equation (3). As with the tortuosity, also the constriction factor is solely dependent on the pore structure and the direction of the voltage drop. Note also that both parameters are scale invariant.

## FONTAINEBLEAU SANDSTONE EXAMPLE

We next investigate four micro-CT images and seven digital rock models of Fontainebleau sandstone with porosities ranging from 8% to 25%. The models were created using the commercial software eCore v.1.5.2. The micro-CT images and models have a sample size of 2.7mm cubed, with a voxel resolution of 5.7µm. The theory introduced above is applied both directly on the voxel grid and on extracted network representations of the pore space.

On the grid representation, we introduced an electrical potential $\Delta U$ over two opposite end-planes of the sample and numerically solved the Laplace equation, Equation (4). On the resulting electrostatic potential field U we tracked electric field lines, and calculated the tortuosity and constriction factor as given by Equations (5) and (7). These results are plotted in Figure 1, while the conducting porosity is plotted in Figure 2. We then obtained

the formation resistivity factor from Equation (3), and the resulting values are plotted in Figure 3. In the same plot we have added experimental Fontainebleau data from [4].

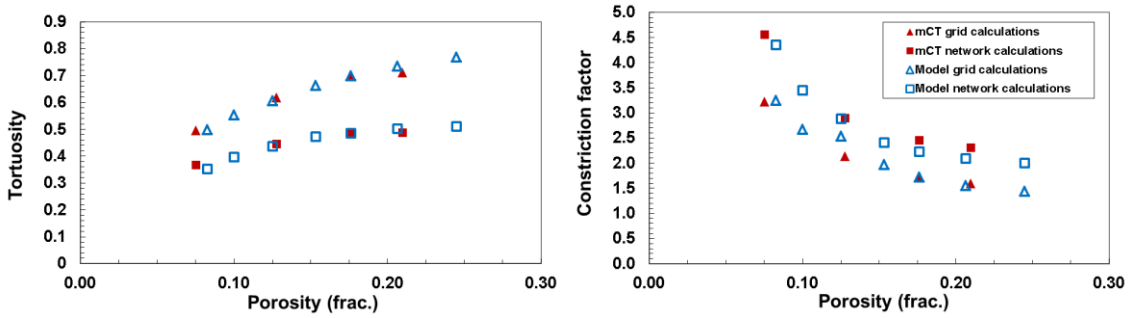


**Figure 1:** Porosity versus tortuosity, $\boldsymbol{\tau_c}$ , in the left plot, and porosity versus constriction factor, $\boldsymbol{C_c}$, in the right plot, for mCT and model samples.

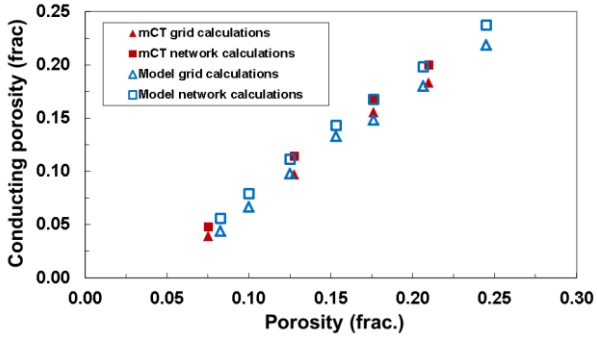


**Figure 2:** Porosity versus conducting porosity, $\boldsymbol{\varphi_c}$, for mCT and model samples.

We extracted networks from both the micro-CT and models, again using eCore v.1.5.2. These networks are a simplified representation of the pore space, with nodes associated to pore bodies and links associated to the pore throats connecting the pore bodies. For each link in the network we associated a resistor of conductance

$$G_t = \sigma\left(\frac{l_1^2\alpha_1}{V_1} + \frac{l_t^2}{V_t} + \frac{l_2^2\alpha_2}{V_2}\right)^{-1}. \qquad (8)$$

Here $l_1$ and $l_2$ is the length between the center of pore 1 and pore 2 respectively and the connection between this pore and link $t$, $l_t$ is the length of link $t$, $V_1$, $V_2$ and $V_t$ is the volume of the pore 1, pore 2 and link $t$ respectively, and $\alpha_1$ and $\alpha_2$ is the number of links connected to pore 1 and pore 2 respectively. All those quantities are produced by the network extraction algorithm. The conductivity $\sigma$ of the brine will not influence our results. Note that the factors $\alpha_1$ and $\alpha_2$ in Equation (8) are not included in commonly used conductance formulations [5, 6]. However, a conductance formulation without $\alpha_1$ and $\alpha_2$ is not volume preserving.

We then numerically solved for the electrical potential in each node using inlet and outlet nodes as fixed boundaries. We calculated the tortuosity and constriction factor as given

by Equations (5) and (7), a full description of the workflow can be found in [2]. These results are plotted in Figure 1, while the conducting porosity is plotted in Figure 2. The calculated values for the formation resistivity factor based on Equation (3) are plotted in Figure 3.

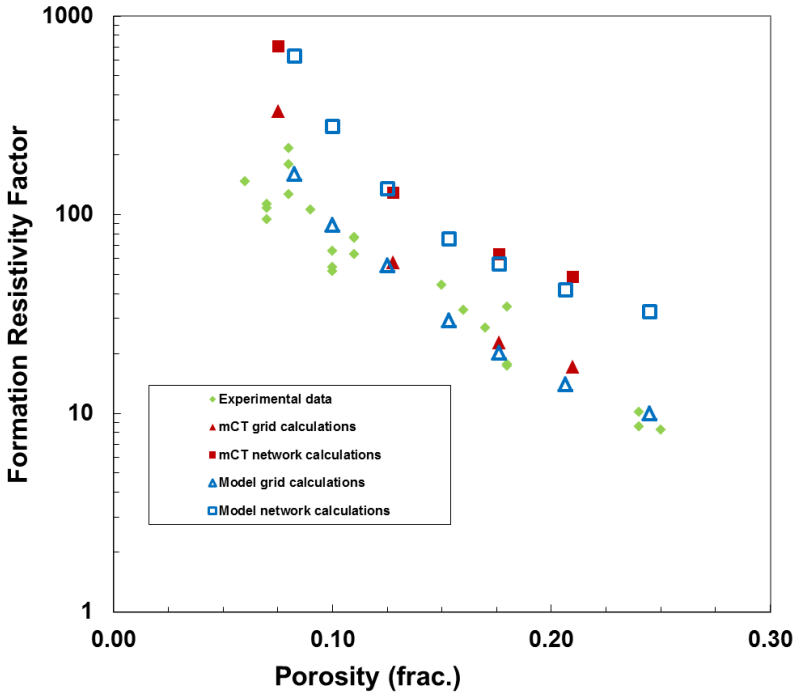


**Figure 3:** Experimental and calculated porosity and formation factor.

## DISCUSSION

As seen from Figure 3, the formation resistivity factors from calculations directly on the grid representation follow the trend of the experimental data, while the formation resistivity factors from calculations on the corresponding network representations differ significantly. This is in contrast with calculations in [6], where the network calculations followed the trend given by experimental data. This discrepancy arises from the fact that our network model is volume conserving, while the network model used in [6] is not.

As seen from Figure 1, there are quantitative differences for both the tortuosity and the constriction factor between grid and network representations. We investigated changing the length $l_i$ in Equation (8) to obtain the same conductance description as used in [5, 6], however, this resulted in a tortuosity larger than 1 for large porosities.

For both the grid and the network calculations, part of the pore space will not contribute to the electrical conductance, as shown in Figure 2. The difference in trends for the network and the grid calculations seen in Figure 2 is assumed not significant, when resolution issues and numerical errors are taken into account.

## CONCLUSION

In this paper, we have presented a microstructure description of the relationship between the formation resistivity factor and the porosity as introduced in [2]. The pore microstructure of the reservoir rock is described by a tortuosity and a constriction factor, whose combined effect determines the formation resistivity factor.

We have applied this theory to micro-CT images and rock models of Fontainebleau sandstone. The calculations indicate that the current standard for network extraction results in network models for which the electrical conductance is inherently different from the electrical conductance on the original grid models. The quantitative differences in the microstructure representations are revealed in the calculated tortuosity and constriction factors.

This theory should be of help in developing network extraction algorithms that preserve the effect of the rock microstructure with regard to electrical conductance. Similarly, rock typing in core analysis could become more tangible when involving fundamental structure-property relations as outlined in this paper.

## BIBLIOGRAPHY

[1] Archie, GE, "The electrical resistivity log as an aid in determining some reservoir characteristics," *Trans. AIMe,* vol. 146, no. 1, pp. 54--67, 1942.

[2] Berg, CF, "Re-examining Archie's law: Conductance description by tortuosity and constriction," *Physical Review E,* vol. 86, no. 4, 2012.

[3] Bear, J, Dynamics of fluids in porous media, Courier Dover Publications, 1972.

[4] Gomez, CT, Dvorkin, J and Vanorio, T, "Laboratory measurements of porosity, permeability, resistivity, and velocity on Fontainebleau sandstones," *Geophysics,* vol. 75, no. 6, pp. E191--E204, 2010.

[5] Valvatne, PH, Predictive pore-scale modelling of multiphase flow, PhD thesis, Imperial College London, 2004.

[6] Øren, PE and Bakke, S and Arntzen, OJ, "Extending predictive capabilities to network models," *SPE Journal,* vol. 3, no. 4, pp. 324--336, 1998.